New Jersey Institute of Technology

Digital Commons @ NJIT

3-31-1972

Studies of rare earth compounds

Rostam Mondegarian
New Jersey Institute of Technology

Recommended Citation

STUDIES

OF RARE EARTH COMPOUNDS

BY

ROSTAM MONDEGARIAN

A THESIS

PRESENTED IN PARTIAL FULFILLMENT OF

THE REQUIREMENTS FOR THE DEGREE

OF

MASTER OF SCIENCE IN CHEMISTRY

AT

NEWARK COLLEGE OF ENGINEERING

NEWARK, NEW JERSEY
1972

APPROVAL OF THESIS

STUDIES

OF RARE EARTH COMPOUNDS

BY

ROSTAM MONDEGARIAN

FOR

DEPARTMET OF CHEMISTRY

NEWARK COLLEGE OF ENGINEERING

BY

FACULTY COMMITTEE

APPROVED:

NEWARK, NEW JERSEY

MARCH, 1972

ABSTRACT

The work reported herein has consisted of miscellaneous studies of rare earth compounds.

1. The Pr-As system was studied with a view to obtaining a ferromagnetic composition.

2. Attempts were made to prepare ternary compounds by solid state reaction of PrAs, GdAs or YbAs with MnAs, CrAs or FeAs, and PrP, GdP, or YbP with MnP, CrP or FeP.

3. Attempts were made to prepare quaternary compounds by solid state reaction of YbAs, YbP and GdAs with CdI_2 in various molar ratios. In many cases new compouns appeared to be formed but because of complexity of the X-ray patterns it was not possible to determine the structure or compositions of these compounds.

In the case of $YbAs+CdI_2$ and $CdI_2+2YbAs$ at 570° C. It was found that the reaction yields a mixture of Cd_3As_2 and YbI_3.

4. Attempts were made to prepare ternary compounds in the systems YbI_3+YbAs and GdI_3+GdAs. In these cases new compounds appeared to be formed but because of the complexity of the X-ray patterns it was not possible to determine the structure or compositions of these compounds.

5. The reflectance spectra of Pr and Nd garnets with rare earths on two crystallographic sites which have been prepared in this laboratory were studied. In one system with Pr on dodecahedral sites, new absorption bands at 350-450 mμ and 490-575 mμ were observed.

The new absorption bands are believed to be due to the presence of small quantities of Pr^{4+} and Yb^{2+} ions by the redox reaction

$$Pr^{3+} + Yb^{3+} \rightleftharpoons Pr^{4+} + Yb^{2+}$$

ACKNOWLEDGEMENT

The author wishes to express his sincere gratitude to Dr. Lawrence Suchow, his research advisor, for his guidance throughout this research project.

TABLE OF CONTENTS

LIST OF TABLES

LIST OF TABLES (CONTINUED)

LIST OF FIGURES

I. PROBLEM STUDIED

The work reported herein has consisted of miscellaneous studies of rare earth compounds.

1.   In the previous unpublished work on praseodymium-arsenic compounds by C. Frasier[1] it appeared that one praseodymium arsenide was ferromagnetic but the preparation was not single-phase. An effort was made to find the composition of this compound and prepare it pure by studying the Pr-As system. It was found, however, that Frasier's sample had been contaminated with metallic iron. Study of the Pr-As system was continued, but in the meantime a paper was published by Taylor et al[2] reporting the study of the binary systems formed between arsenic and praseodymium, terbium, holmium, yttrium, lanthanum, cerium, neodymium, gadolinium and ytterbium. Although considerable work had been carried out on the Pr-As system and attempts had been made to calculate lattice constants for the compounds formed, this effort was discontinued.

2.   Attempts were made to prepare ternary compounds by solid state reactions of PrAs, GdAs, or YbAs with MnAs, CrAs, or FeAs, and PrP, GdP, or YbP with MnP, CrP or FeP.

3.   Attempts were made to prepare quaternary compounds

by solid state reaction of YbAs, YbP and GdAs with CdI_2 in various molar ratios.

4. Attempts were made to prepare ternary compounds in the system YbI_3-YbAs and GdI_3-GdAs.

5. The reflectance spectra of praseodymium and neodymium garnets with rare earths on two crystallographic sites which have been prepared in this laboratory[3] were studied.

II. RELEVANT CRYSTAL STRUCTURES

Perhaps the most relevant crystal structures are those of NaCl, Th_3P_4, ZnS, and spinel.

IIA. NaCl Structure[4]

The largest group of RX type crystals have the structure of sodium chloride, NaCl. The R can be one of the rare earth elements and the X one of the other elements in the periodic table. The unit arrangement of NaCl contains four molecules with atoms in the positions:

R: (4a)   0 0 0; 1/2 0 1/2; 1/2 1/2 0; 0 1/2 1/2,
            or 0 0 0; F.C.

X: (4b)   1/2 1/2 1/2; 1/2 0 0; 0 1/2 0; 0 0 1/2
            or 1/2 1/2 1/2; F.C.

Each R atom has six equidistant X atoms as nearest neighbors, and vice versa. Since these neighbors are at the corners of a regular octahedron, this is referred to as octahedral coordination.

Compounds of the following chemical types crystallize with the NaCl arrangement:

A. Alkali and silver halides and alkali pseudohalides.

B. Alkaline earth oxides, sulfides, selenides and tellurides.

C. Nitrides, phosphides and other fifth column binary compounds with trivalent metals (chiefly rare earths) such as:

CeAs, CeBi, CeN, CeP, DyP, PrAs, HoAs HoBi, GdAs, and others.

D. Carbides of various metals.

IIB. SPINEL STRUCTURE[5,6]

The name, spinel structure is from the compound which occurs in nature with composition $MgAl_2O_4$.

The general chemical formula for compounds which may crystallize in the spinel structure is MQ_2X_4. X is a non-magnetic anion which may be sulphur or selenium or, as is the case in the great majority of cases studied, oxygen. M is a cation of a metal such as Mn, Fe, Ni, Co. In the normal spinel the Q cations (such as those of Fe, Al, or Ga) are in the octahedral interstices and M is the ion in the tetrahedral sites.

An important variant is the inverse spinel structure in which half of the Q ions are in tetrahedral interstices and the M ions are in the octahedral ones along with half of the Q ions. This often happens when the M ions have a stronger preference for octahedral coordination than do the Q ions.

M and Q are the magnetic ions in a ferromagnetic spinel. The spinel compounds containing iron, i.e. MFe_2O_4, are generally called ferrites and form a large and widely used group which includes the simplest ferrimagnetic compound, magnetite, Fe_3O_4. Examples of spinel ferrites are $MnFe_2O_4$, $NiFe_2O_4$, and $MgFe_2O_4$.

The spinel structure also exists where the X is a sulfide or selenide ion. Suchow and Stemple[7] reported the spinels in which the octahedral sites were occupied by rare earth ions, e.g. CdY_2S_4, $CdTm_2S_4$, $CdDy_2Se_4$, CdY_2Se_4.

There are several other rare earth thiospinels[8] and selenospinels of which there is a transition metal ion in addition to the rare earth ions with unpaired electrons. These spinels are $MnYb_2S_4$, $MnYb_2Se_4$, $FeYb_2S_4$, and $MnTm_2S_4$. Longo and Raccah[9] have investigated the magnetic properties of $MnYb_2S_4$ and the magnetic properties of $FeYb_2S_4$, and $MnYb_2Se_4$ have been studied by Suchow and Ando[10].

IIC. Th₃P₄ STRUCTURE

The structure of thorium phosphide was determined
by Meisel in 1939[11] and has been completely described
by others[12,13].

This structure fits the I43d space group (Hermann-
Mauguin symbol) and T_d^6 (Schoenflies symbol)[14] with site
symmetry of $2S_4$ (12), C_3 (16), C_2 (24), (A site), (C_3 is
a three fold axis, $2S_4$ are two rotation-reflection axes,
i.e. rotation about axis by 360/4 degrees followed by
reflection in a plane perpendicular to the axis, C_2 is
a two fold axis, and since in the cubic case we have
three faces,(i.e. A, B, C), A in this structure means
A site of cubic has been centered).

The phosphorus atoms occupy 16 general positions,
determined by a parameter u. The 12-fold Th positions
are fixed by the space group. The maximum coordination
of 8 around Th is obtained for u=1/2. Atoms have been
placed in the following special positions[15]:

Th: (12a)   3/8 0 1/4; 1/8 0 3/4; 3/4 1/8 0;
                1/4 3/8 0; 0 1/4 3/8; 0 3/4 1/8; B.C.

P :   (16c)   uuu;   u,u,1/2-u;
                1/2-u,u,u   u,1/2-u,u;
                u+1/4,u+1/4,u+1/4; 1/4-u,u+1/4,3/4-u;
                u+1/4,3/4-u,1/4-u; 3/4-u,u+1/4,1/4-u; B.C.

For different compounds with Th_3P_4 structure there
is a different value u and for Th_3P_4 itself u is equal
0.083 Å. In this structure each thorium atom has about
eight phosphorus atoms at a distance of 2.98 Å. The
nearest approach of phosphorus atoms to one another is
3.20 Å.

In contrast to the regular NaCl octahedron the
Th_3P_4 polyhedron has no center of symmetry and there is
only one three fold rotation axis. It exists in left
and right-handed forms depending on the distribution of
the three elongations over the 12 octahedral edge. In
the fcc packing of the NaCl Structure (Fig.I), the
octahedra share edges, and the empty spaces between
the faces of neighboring octahedra form regular tetrahedra.

O: Na

●: Cl
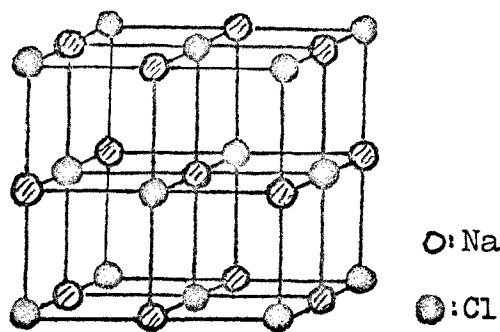
Fig. I. The sodium chloride structure

The Th_3P_4 octahedra, however, share faces with only three
empty irregular tetrahedra.

Many rare earth compounds crystallize in the Th_3P_4 structure. It has been also reported that Gd_4Bi_3, Gd_4Sb_3,[16] and Yb_4Sb_3[17] have the anti-Th_3P_4 structure. Gambino[18] reported that the Gd_4Bi_3 structure is formed by all the lighter rare-earth elements with antimony and bismuth. The lattice constants of these compounds vary linearly with the ionic radii of the rare earth elements. All the Gd_4Bi_3 structure compounds found in these systems have ratios between 0.4175 and 0.5129. Europium, ytterbium and, to a slight extent, samarium are divalent in the Gd_4Bi_3 structure.

The structure and lattice constant of the 4:3 compositions studied are shown in Table I. It will be seen from these results that the Gd_4Bi_3 structure is found in all RE_4Sb_3 compositions for the elements La through Dy, with the exception of europium, and all RE_4Sb_3 (Table II) compositions for the elements La through Gd. Ytterbium forms the Gd_4Bi_3 structure with both Sb and Bi.

Table I. $(RE)_4Bi_3$ Compounds.   R.J. Gambino, <u>J. Less-Common Metals</u>, <u>12</u>, 346 (1967)

Composition	Structure	Lattice Constant $a(\mathring{A})$	Comments	Ref.
La_4Bi_3	Gd_4Bi_3	9.759		22
Ce_4Bi_3	Gd_4Bi_3	9.640		"
Pr_4Bi_3	Gd_4Bi_3	9.600		"
Nd_4Bi_3	Gd_4Bi_3	9.550		"
Sm_4Bi_3	Gd_4Bi_3	9.814		"
Eu_4Bi_3	Gd_4Bi_3	10.00		"
Gd_4Bi_3	Gd_4Bi_3	9.383		16
Tb_4Bi_3	–	–	Not studied	"
Dy_4Bi_3	Not formed	–	Two phases, $DyBi+Dy_3Bi_2$	"
Ho_4Bi_3	–	–	Not studied	"
Er_4Bi_3	–	–	Not studied	"
Tm_4Bi_3	Not formed	–	Multiphase product, TmBi major phase	

Table I. (Continued)

Composition	Structure	Lattice Constant a($\overset{\circ}{A}$)	Comments	Ref.
Yb_4Bi_3	Gd_4Bi_3	9.520		11
Yb_4Bi_3	-	-	Not studied	12

Table II. $(RE)_4Sb_3$ Compounds. R.J. Gambino, <u>J. Less-Common Metals</u> <u>12</u>, 346 (1967).

Composition	Structure	Lattice Constant a(Å)	Comments	Ref.
La_4Sb_3	Gd_4Bi_3	9.630		22
Ce_4Sb_3	Gd_4Bi_3	9.511		"
Pr_4Sb_3	Gd_4Bi_3	9.360		"
Nd_4Sb_3	Gd_4Bi_3	9.380		"
Sm_4Sb_3	Gd_4Bi_3	9.300		"
Eu_4Sb_3	Not formed	–	Two phase product	"
Gd_4Sb_3	Gd_4Bi_3	9.224		12
Tb_4Sb_3	Gd_4Bi_3	Not determined	Weak Gd_4Bi_3 lines observed as second phase; TbSb major	12
Dy_4Sb_3	Gd_4Bi_3	9.12		12
Ho_4Sb_3	Not formed	–	Two phases, HoSb major phase	"
Er_4Sb_3	Not formed	–	Two phases, ErSb major phase	"
Tm_4Sb_3	Not formed	–	Two phases, TmSb major phase	"

Table II. (Continued)

Composition	Structure	Lattice Constant a(Å)	Comments	Ref.
Yb_4Sb_3	Gd_4Bi_3	9.300		17
Y_4Sb_3	Gd_4Bi_3	9.090	Observed as a second phase	"
Gd_4As_3	Not formed	–	GdAs+Gd	"
Dy_4As_3	Not formed	–	DyAs+Dy	"

In the Gd_4Bi_3 structure the rare earth occupies the phosphorus site and the other element the thorium sites in Th_3P_4. The crystal chemical factors which favor the formation of Th_3P_4 structure have been discussed by Flahaut[19] who has shown that only the large rare earth elements form the normal Th_3P_4 or closely-related structures which fall into four classes as shown in Table III.

Table III. R.J. Gambino, J. Less-Common Metals, 12, 350, (1967). Th_3P_4-Type Structures

Type	General Formula	Examples	Ref.
Th_3P_4	A_3X_4	Th_3P_4, La_3S_4	19
Defect Th_3P_4	A_2X_3	La_2S_3 or $La_{3-x}S_4$	19
Gd_4Bi_3	A_4X_3	Ga_4Bi_3	18
		Yb_4Bi_3	16
Pu_2C_3	A_2X_3 or	Pu_2C_3	20
Anti-Th_3P_4	$A_4(X_2)_3$	Rb_4O_6, Cs_4O_6	21

It has been observed that most systems which form compounds with the Th_3P_4 structure also contain a 1:1 compound with the NaCl structure that will be discussed later.

III. <u>RARE-EARTH ARSENIDES</u>

IIIA. <u>Introduction</u>

In previous unpublished work on rare earth arsenides, C. Frasier[1] reported a ferromagnetic praseodymium-arsenic compound, but it was not single-phase. In the present work, attempts were made to prepare this compound pure.

A few binary rare earth compounds with different structures have been reported by Vogt, Hulliger, and others as ferromagnetic compounds. It was supposed that Frasier's sample had a structure similar to one of these ferromagnetic compounds.

Hulliger and Vogt[23] have reported Eu_3P_2 and Eu_3As_2 as new ferromagnetic compounds. They have reported that the crystal structure of Eu_3P_2 and Eu_3As_2 is body-centered cubic of the Ba_3P_2 type[24] which is a Gd_4Bi_3 anti-Th_3P_4 type with 1/9 of the anion sites empty:

$$Eu_{16}P_{10\ 2/3}\ \square\ _{4/3}$$
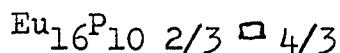
Each Eu is surrounded by six anions and it forms a distorted octahedron in which the Eu-P distance is 2.95Å for one phosphorus and 3.31 for the other one in the phosphide while the anions are coordinated

by the octaverticon (a strongly twisted cube) of cations. In the phosphide each Eu atom has three Eu neighbors as close as 3.54Å, two at 3.91Å and six at a distance of 4.25Å.

Both Eu_3P_2 and Eu_3As_2 obey a Curie-Weiss law and become ferromagnetic at low temperature.

Curie-Weiss law: $\chi_M = \dfrac{C_M}{T-\theta}$,

where χ_M is molar magnetic susceptibility, C_M the molar Curie constant, T the absolute temperature, and θ the Weiss constant.

The molar susceptibility, χ_M, is the sum of the gram-atom susceptibilities, and the molar Curie constant, C_M, the sum of individual gram-atom Curie constants of all atoms or ions in the formula unit of a compound. The individual gram-atom Curie constant for an atom or ion is related to the effective magnetic moment in Bohr magnetons, μ_{eff}, by the expression,

$$\mu_{eff} = 2.84 \sqrt{C_{M(ind)}},$$

which derives from the Langevin formula. Superimposed diamagnetic susceptibility is usually neglected.

Calculated values of μ_{eff} (in Bohr magnetons) of ions are obtained from the expression,

$$\mu_{eff} = g\sqrt{J(J+1)}$$

For transition metal ions, J is often due to spin only so that

$$\mu_{eff} = g\sqrt{S(S+1)}$$

Table IV summararizes all the magnetic data for Eu_3P_2 and Eu_3As_2.

Table IV. Crystallographic and Magnetic Data of Eu_3P_2 and Eu_3As_2. Hulliger, F., Vogt, O., <u>Solid State Communications</u>, <u>8</u>, 772 (1970).

	a(Å)	χ_{Eu}	$\theta p(°K)$	$n_p(\mu Bohr)$	$T_c(°K)$	$n_f(\mu Bohr)$ at 1.5°K
Eu_3P_2	9.026	0.065	33	7.9	25	6.8
Eu_3As_2	9.225	0.067	23	8.0	17.5	7.0

In this table, θ_p is the paramagnetic Curie temperature, n_p the effective magneton number, T_c the ordering temperature, and n_f the magnetic number in the ferromagnetic state determined with pulsed fields at 1.5°K.

Holtzberg, et al[25] have studied the structural, electrical, and magnetic properties of the matallic 4:3 compounds and the 2:3 rare-earth semiconductors with specific reference to gadolinium.

According to Holtzberg's report, Gd_4Sb_3, Gd_4Bi_3 are both ferromagnetic compounds with the structure of inverted Th_3P_4; i.e., the rare earth atoms occupy the 16-fold P sites. Therefore, the rare-earth atoms have 6-fold coordination. The lattice constant of Gd_4Sb_3 and Gd_4Bi_3 are 9.22 and 9.38Å respectively. The shortest distance, 3.49Å, between Gd atoms in Gd_4Bi_3, which has the largest lattice constant, is approximately 2% shorter than the nearest neighbor distance in Gd metal. The compounds Gd_4Sb_3 and Gd_4Bi_3 are completely soluble in one another. All $Gd_4(Sb_xBi_{1-x})_3$, (x=0, 1/4, 1/2, 3/4 or 1) are ferromagnetic at low temperatures, and the Curie temperature T_C varies in the solid solution system Gd_4Sb_3-Gd_4Bi_3 with composition from 260 to $340°K$.

The Curie temperature for Gd_4Bi_3($T_C=340°K$) is higher than in Gd metal ($290.7°K$) and decreases rapidly with increasing Sb concentration. Some properties of Gd compounds of several compositions are shown in Table V.

The 2:3 compounds of trivalent rare earths with divalent sulfur and selenium anions represent a Th_3P_4 structure with the rare earth atoms in 8-fold coordination. The deviation from the 3:4 composition

which is necessary for charge balance in the semi-
conducting compound results in a defect lattice
having 4/3 disordered vacancies in the 12 Gd sites
per unit cell[26]. This structure has, as a conse-
quence, a relatively wide range of Gd or similar
atoms in the defect lattice[27]. The increasing ex-
cess of trivalent metal supplies the material with
donors for conduction electrons, resulting in a
continuous change from semiconducting to a metallic
character. The stoichiometric 2:3 compound (Gd_2Se_3)
is a semiconductor with an electrical resistivity at
room temperature, $\rho = 3 \, \Omega$ cm, having a negative tempera-
ture coefficient of resistivity.

With increasing Gd content up to $Gd_{2.1}Se_{2.9}$ the
system retains the Th_3P_4 structure with no measurable
changes in the lattice constant. At higher Gd concen-
tration the 1:1 rock salt compound precipitates. The
increase in Gd concentration results in an increase of
electrical conductivity (decrease in electrical
resistivity) and also raises the paramagnetic Curie
temperature. As soon as θ_p becomes positive the
samples show ferromagnetism. Table V shows some pro-
perties of Gd compounds of several composition.

It was supposed that the praseodymium arsenide
compound that was discussed has some vacancies and

structure similar to one of these ferromagnetic
compounds. Attempts were made with different ratios
of Pr:As and different temperatures for various lengths
of time to prepare the compound pure. Finally, it
was found by spectrographic and x-ray diffraction
analysis that Frasier's preparation was contaminated
with metallic iron, which was the ferromagnetic
material.

Table V. Lattice Constant (a_0), Electrical Resistivity (ρ), Paramagnetic Curie Temperature (Θ_ρ), and Effective Moment (n_{eff}) per Gd Atom for Compounds of Several Compositions.

	a_0 (Å)	ρ (ΩCm) at room temp.	Θ_ρ (K)	n_{eff} (μ)
$Gd_{2.0}Se_{3.0}$	8.718		-10	7.75
$Gd_{2.1}Se_{2.99}$	8.718	3.4	-16	7.63
$Gd_{2.05}Se_{2.95}$	8.718	0.2	+3	7.96
$Gd_{2.7}Se_{2.93}$	8.718	...	+17	7.68
$Gd_{2.08}Se_{2.92}$	8.718	3.1×10^{-2}	+30	7.93
$Gd_{2.09}Se_{2.91}$	8.718	2.0×10^{-3}	+65	8.01
$Gd_{2.10}Se_{2.90}$	8.718	1.4×10^{-3}	+88	7.74

Besides attempting to prepare the compound reported by Frasier, the entire binary system Pr-As was examined. In the meantime, a paper was published by Taylor et al[2], reporting the study of the binary compounds formed between arsenic and Pr, Y, La, Ce, Nd, Gd, Tb, Ho and Yb. Therefore, work on the Pr-As system was discontinued.

The binary systems of rare earth elements with arsenic have been investigated and the crystallographic data for the various phases are reported.

AB phases: It has been found that all the binary systems, A-As (where A is a rare earth element), have a phase at the equiatomic composition which crystallizes in the NaCl structure. Equiatomic compounds formed with lanthanide elements except europium have been known for some time[28,29]. Bruzzone[30] reported EuAs as "non-cubic" but Craven and Ostertag[31] prepared an NaCl-type equiatomic europium arsenide by reacting europium with arsenic triiodide in liquid ammonia. The only structure observed for equiatomic compounds of the rare earths with group VB elements is NaCl type although there is an indication that above 400 degrees Centigrade LaSb may transform from the f.c.c. to a primitivo lattico[32].

Observations in the present work indicated a

NaCl-type structure for PrAs. Lattice parameter determination is in agreement with previous reports. The lattice constant of rare earth arsenides with NaCl-type structure is given in Table VI.

AB$_2$ phases: AB$_2$ phases are not unknown in the rare earth-VB systems. La, Ce, Pr, Nd, Sm, Gd, and Tb antimonides all crystallize with the LaSb$_2$-type structure and YbSb$_2$ with the ZnSi$_2$-type[33,34]. Wang et al.[35] have reported the lattice parameters of LaSb$_2$, CeSb$_2$, NdSb$_2$, and SmSb$_2$ (see Table VII) and Eatough et al[36], have reported the lattice parameters of a few rare earth diantimonide compounds (see Table VIII).

After the NaCl type structure in rare earth arsenides, the most frequently occurring structure type is the NdAs$_2$ type which has been found by Taylor et al[2], and it has been reported for the diarsenides of La, Ce, Pr, and Nd. Single crystal measurements have indicated that the symmetry is monoclinic:

LaAs$_2$ (below 750°C) a=4.212Å, b=6.935Å, c=10.647Å, β=106.60°
PrAs$_2$ a=4.139Å, b=6.844Å, c=10.509Å, β=106.69°
CeAs$_2$ a=4.165Å, b=6.871Å, c=10.561Å, β=106.72°
NdAs$_2$ a=4.109Å, b=6.819Å, c=10.449Å, β=106.68°

Table VI. Rare Earth Compounds With the NaCl Structure
From Wyckoff Crystal Structures 1, 88-89, (1963)
Interscience Publishers.

Crystal	Lattice Constant a_0(Å)
LaAs	6.125
CeAs	6.066
PrAs	5.997
NdAs	5.958
SmAs	5.921
GdAs	5.854
TbAs	5.813
DyAs	5.780
HoAs	5.771
ErAs	5.732
TmAs	5.711
YbAs	5.698

Observations in the present work were in agreement with Taylor's work on $PrAs_2$ but the lattice parameters were not determined.

Table VII. Crystal Data of $LaSb_2$, $NdSb_2$, and $CeSb_2$ From R. Wang, <u>Inorg. Chem</u>., <u>6</u>, 1689 (1967).

	$a_o(\text{Å})$	$b(\text{Å})$	$c(\text{Å})$
$LaSb_2$	6.314 ± 0.005	6.175 ± 0.005	18.56 ± 0.01
$CeSb_2$	6.295 ± 0.006	6.124 ± 0.006	18.21 ± 0.02
$NdSb_2$	6.207 ± 0.004	6.098 ± 0.004	18.08 ± 0.01
$SmSb_2$	6.051 ± 0.006	6.051 ± 0.006	17.89 ± 0.02

Table VIII. Lattice Parameters of Rare Earth Diantimonides
From N. L. Eatough, Inorg. Chem., 8, 1445, (1964).

	$a(Å)$ LaSb$_2$-Type	$b(Å)$ (8 molecules/Unit Cell)	$c(Å)$
PrSb$_2$	6.230 ± 0.006	6.063 ± 0.006	17.89 ± 0.02
NdSb$_2$	6.230 ± 0.004	6.063 ± 0.004	17.89 ± 0.02
GdSb$_2$	6.157 ± 0.002	5.986 ± 0.002	17.83 ± 0.01
TbSb$_2$	6.123 ± 0.006	5.969 ± 0.006	17.72 ± 0.02

High Pressure Orthorhombic Type (Two Molecules/Unit Cell)

GdSb$_2$	5.930 ± 0.003	3.296 ± 0.002	8.030 ± 0.004
TbSb$_2$	5.903 ± 0.003	3.282 ± 0.002	7.990 ± 0.004
DySb$_2$	5.888 ± 0.003	3.273 ± 0.002	7.965 ± 0.004
HoSb$_2$	5.874 ± 0.002	3.266 ± 0.001	7.939 ± 0.003
ErSb$_2$	5.866 ± 0.006	3.259 ± 0.003	7.926 ± 0.008
TmSb$_2$	5.851 ± 0.002	3.252 ± 0.001	7.912 ± 0.004
YbSb$_2$	5.907 ± 0.003	3.283 ± 0.002	7.981 ± 0.004

A_4B_3 phase: There are just three binary rare earth arsenides with the stoichiometry of 4:3. Pr_4As_3 and Ce_4As_3 have been reported by Parthe[37] with anti-Th_3P_4 structure and the following lattice constants:

$$Ce_4As_3 \quad a=9.052\pm0.001\overset{\circ}{A}$$
$$Pr_4As_3 \quad a=8.984\pm0.004\overset{\circ}{A}$$

The only other arsenide which has been found with stoichiometry of 4:3 and with the anti-Th_3P_4 structure is Yb_4As_3[38]. Many rare earth antimonides and bismuthides with 4:3 stoichiometry are known and they all have the anti-Th_3P_4 structure[38,39]. Table IX contains crystallographic data for the rare earth arsenide that have been reported by Taylor et al[2].

Table IX. Lattice Parameters of Rare-Earths Arsenides.
From J.B., Taylor, _J. Less-Common Metals_, _22_, 53 (1970)

Phase	Structure Type	Lattice Constant
Yb_5As_3	Mn_5Si_3 (Yb-rich)	a=8.480Å, c=6.671Å, c/a=0.787
	(As-rich)	a=8.445Å, c=6.618Å, c/a=0.784
Ce_4As_3	anti-Th_3P_4	a=9.053Å
Pr_4As_3		a=8.994Å
Yb_4As_3		a=8.791Å
Yb_4As_3	deformed anti-Th_3P_4	a=8.784Å, α=90.80°
REAs	NaCl	shown in Table VI.
$LaAs_2$ (above 750° C)	$LaAs_2$	a=12.891Å, b=9.140Å, c=14.450Å, γ=135.16°
$LaAs_2$ (below 750° C)	$NdAs_2$	a=4.212Å, b=9.935Å, c=10.647Å, β=106.72°
$CeAs_2$	$NdAs_2$	a=4.165Å, b=6.871Å, c=10.561Å, β=106.72
$PrAs_2$	$NdAs_2$	a=4.139Å, b=6.844Å, c=10.509Å
$NdAs_2$	$NdAs_2$	a=4.109Å, b=6.819Å, c=10.449Å, β=106.68°

IIIB. <u>Preparation</u>

Praseodymium arsenides were prepared by solid-gas reaction of stoichiometric mixture of praseodymium[a] and arsenic[b] in evacuated and sealed quartz tubes.

The procedure was as follows:

1. A vacuum was drawn on the tube and the evacuated tube brought into a dry box and filled with dry nitrogen. The reaction tube was weighed.

2. Under dry nitrogen in a dry box the praseodymium was washed with hexane three times to remove the protective oil.

3. Praseodymium was weighed into the quartz reaction tube.

4. A stoichiometric amount of arsenic was weighed and it was added to the reaction tube.

5. A vacuum was drawn on the tube for five minutes to remove any air which might oxidize praseodymium. To insure the complete removal of air from the tube, the tube was then flushed with argon. This process

---

[a]Bernard Ring, Inc., New York, N.Y. (99.9%).
[b]City Chemical Corporation New York, (99%).

was repeated three times followed by a final five minute evacuation. After this period, the tubes were sealed using an oxygen-natural gas torch.

6. The tubes were put into a muffle furnace at room temperature and the temperature was raised. For different compounds, different temperatures and various heating periods were used (see Table X).

7. The tubes were cooled by air-quenching at room temperature.

8. Compounds were ground into fine powder and analyzed by the X-ray diffraction powder method using Norelco equipment with 57.3-mm powder cameras.

IIIC. Results

The experimental results on the Pr-As system are given in Table X. Lattice constants in the table are from previous work on this system because, in the present work, the lattice parameters were not determined and just the phases observed in this work were compared with those from previous studies. Observations in the present work are in agreement with previous work.

Table X. Temperatures and Time Periods Required for Preparation of Pr-As Compounds and Crystallographic Data of These Compounds (Nominal Compositions)

Nominal Composition	Time and Temperature	Structure	Lattice Constant	Ref.
$PrAs_2$	4 hrs. at 450° C, Overnight at 800° C.	Monoclinic	$a=4.139Å$, $b=6.844Å$, $c=10.509Å$, $\beta=106.69°$	2
Pr_2As_3	4 hrs. at 450° C, Overnight at 800° C.	NaCl-phase + extra lines	—	—
Pr_3As_4	4 hrs. at 450° C. Overnight at 800° C.	NaCl-phase + extra lines	—	—
$PrAs*$	4 hrs. at 450° C. Overnight at 800° C.	NaCl	$a=5.997Å$	Table VI.
Pr_4As_3	4 hrs. at 350° C. Overnight at 1200° C.	Anti-Th_3P_4	$a=8.984\pm0.004Å$	37
Pr_3As_2	4 hrs. at 450° C. Overnight at 800° C.	NaCl-phase + extra lines	—	—
Pr_2As	4 hrs. at 450° C. Overnight at 800° C.	NaCl-phase + extra lines	—	—
Pr_3As	4 hrs. at 450° C. Overnight at 800° C.	NaCl-phase + extra lines	—	—

*In the present work PrAs was the only compound whose lattice parameters were determined.

IIID. DISCUSSION

The purpose of the work on Pr-As system was to obtain a compound that is ferromagnetic. Attempts to prepare such a compound failed for the reason given above, but work on the Pr-As system was continued, and the results are shown in Table X. (In this table the lattice constants are those that have been reported by others[2,37]).

Observations in the present work are in agreement with previous work on the Pr-As system. In this work the lattice parameter determined for PrAs (a=6.00Å) (Table XI) is almost the same as the data in the literature (a=5.997Å).

Table XI. X-ray Diffraction Powder Patterns of PrAs (a=6.00A) (Cu Kα Radiation, 57.3-mm. Radius Camera).

hkl	d,Å.	Intensity[a]
110	3.00	s
220	2.12	s
222	1.74	s-
400	1.50	w
420	1.345	s-
422	1.225	s-
440	1.060	vw

[a]Intensity abbreviation: s, strong; w, weak; vw, very weak.

Table XI (Continued)

hkl	d, Å.	Intensity[a]
442 600	1.00	w
620	0.955	w
622	0.905	w
642	0.806	s-

[a]Intensity abbreviation: s, strong; w, weak; vw, very weak.

IV. TERNARY SYSTEMS

IV A. Introduction

This work was initiated in an attempt to synthesize new complex compounds by solid state reaction of PrAs, PrP, GdAs, YbAs, and YbP (having the NaCl structure) with FeAs, FeP, MnAs, CrAs, and CrP (having the NiAs structure[40]).

In the NiAs structure[41], each atom has 6 nearest neighbors of the other sort, but the arrangement of the neighboring atom is different for the two kinds of atom. An arsenic atom is surrounded by six Ni atoms at the apices of a trigonal prism. The immediate neighbors of a Ni atom are six As atoms arranged octahedrally, but there are also two Ni atoms sufficiently near to be considered bonded to the first Ni atom, as may be seen from the interatomic distances in some compounds with this structure:

| Compound MX | Distance from M to X and M | |
	6X	2M
NiAs	2.43 Å.	2.52 Å.
CoTe	2.62	2.68
NiTe	2.64	2.68

Compound MX	Distance from M to X and M	
	6X	2M
CrSb	2.74 Å	2.73 Å
CoSb	2.58	2.60

From the above figures it will be seen that in the more metallic systems with this structure these eight neighbors are approximately equidistant from the transition metal atom. The ideal NiAs structure has been assigned, often on the evidence of X-ray powder photographs only, to many phases MX in which M is a transition metal and X comes from one of the later B sub-groups (Sn, As, Sb, Bi, S, Se, Te).

Since the rare earth arsenides have the NaCl structure, and 1:1 arsenides and phosphides of Cr, Mn, and Fe have the NiAs structure, it appeared possible that these compounds with two different structures could undergo solid state reaction with each other to produce new compounds. The attempted reactions and results are given in Tables XII and XIII.

IVB. PREPARATION

The required binaries (MnAs, MnP, CrAs, CrP, FeAs,
FeP, PrAs, PrP, YbAs, YbP, GdAs, GdP), were first pre-
pared by reaction between stoichiometric quantities
of pure metal turnings (Yb, Gd, Pr), powder (Mn, Cr)
or wire (Fe), and elemental arsenic or phosphorus in
evacuated sealed quartz tubes. Except for praseo-
dymium arsenide which had been prepared before (the
method of preparation has been discussed above in the
praseodymium arsenides section), the compounds were
prepared in the following manner:

1. Stoichiometric amounts of elements were
weighed and put into a quartz reaction tube.
2. A vacuum was drawn on the tube for five
minutes to remove any air which might oxidize
the elements. To insure the complete removal
of air from the tube, the tube was then flushed
with argon. This process was repeated three
times followed by a final five minutes evacuation.
After this period, the tube was sealed using an
oxygen-natural gas torch.
3. The tubes were put in the furnace at room
temperature and the temperature was raised
(different temperatures and times for different
reactions).

4. The tubes were cooled by air-quenching at room temperature.

5. Compounds were ground into fine powder and analyzed by the X-ray diffraction method using Norelco equipment with 57.3-mm powder cameras.

Following this, stoichiometric amounts of the binaries were thoroughly ground together and caused to react with each other in evacuated, sealed quartz tubes with different times and different temperatures for each compound. The tubes were cooled by quenching in cold water.

All binary and ternary compounds prepared were checked by X-ray diffraction using Norelco equipment with 57.3-mm powder cameras.

IVC. RESULTS

All binary compounds used in this work have been prepared previously and their crystallographic data previously reported. Table XII shows the temperature and times for preparation of the compounds that were synthesized in this laboratory. Crystal structures given are those which have been reported in the literature.

Table XII. The Temperature and Time Required for Preparation of Binary Compounds, and Crystal Structures Data of These Compounds.

	Time and Temperature	Structure	Ref.
CrAs	4 hrs. at 450° C. Overnight at 1000° C.	Distorted NiAs	42
CrP	4 hrs. at 450° C. Overnight at 1000° C.	Distorted NiAs	42
FeAs	4 hrs. at 450° C. Overnight at 1000° C.	Distorted NiAs	42
FeP	4 hrs. at 450° C. Overnight at 1000° C.	Distorted NiAs	42
MnAs	4 hrs. at 450° C. Overnight at 1000° C.	Distorted NiAs	42
MnP	4 hrs. at 450° C. Overnight at 1000° C.	Distorted NiAs	42
GdAs	4 hrs. at 450° C. Overnight at 1000° C.	NaCl	43
GdP	4 hrs. at 450° C. Overnight at 1000° C.	NaCl	43
PrAs	4 hrs. at 450° C. Overnight at 800° C.	NaCl	43
PrP	4 hrs. at 450° C. Overnight at 1000° C.	NaCl	43
YbAs	4 hrs. at 450° C. Overnight at 1000° C.	NaCl	43
YbP	4 hrs. at 450° C. Overnight at 1000° C.	NaCl	43

Attempts were made to prepare a new compound by reaction of binary compounds having a distorted NiAs structure with compounds having the NaCl structure. Attempts to prepare such a compound failed. Table XIII summarizes the attempts which have been made.

Table XIIIA. Arsenic Systems

Reaction Attempted	Time and Temperature	Results
GdAs-MAs Systems		
GdAs-FeAs	1 hr. at 350° C. Overnight at 1000° C.	Mixture of GdAs+FeAs
GdAs-FeAs	3 hrs. at 370° C. Overnight at 1000° C.	
GdAs-MnAs	24 hrs. at 1100° C.	Mixture of GdAs+MnAs
GdAs-CrAs	24 hrs. at 1100° C.	Mixture of GdAs+CrAs
PrAs-MAs Systems		
PrAs-FeAs	Overnight at 1200° C.	Contains FeAs lines and also appears to contain d-spacing shift (perhaps due to solid solution), also many other lines.
PrAs-MnAs	24 hrs. at 1100° C.	Mixture of PrAs+MnAs
PrAs-CrAs	24 hrs. at 1100° C.	Mixture of PrAs+CrAs

Table XIIIA. <u>Arsenic Systems</u> (Continued)

Reaction Attempted	Time and Temperature	Results
	<u>YbAs-MAs Systems</u>	
YbAs-FeAs	Overnight at 1200° C.	Appears to contain all the FeAs lines + many other lines including the YbAs lines but many others too.
YbAs-MnAs	Overnight at 1200° C.	Appears to contain all the MnAs lines + all the YbAs lines (those which truly belong to pure YbAs) and also containing some changes (new lines or may be absence of old lines seen in the unpure YbAs)
YbAs-CrAs	Overnight at 1200° C.	Appears to contain all the CrAs lines and all the YbAs lines.

Table XIIIB. Phosphorus Systems

Reaction Attempted	Time and Temperature	Results
GdP-MP Systems		
GdP-FeP	1 hr. at $350°$ C. Overnight at $1000°$ C. 3 hrs. at $350°$ C. Overnight at $1200°$ C.	Appears to contain all the GdP lines and all the FeP lines.
GdP-MnP	Overnight at $1100°$ C.	Appears to contain the GdP lines and all the MnP lines.
GdP-CrP	Overnight at $1100°$ C.	Appears to contain all the GdP lines and all the CrP lines.
PrP-Mp Systems		
PrP-FeP	24 hrs. at $1100°$ C.	Appears to contain the PrP lines and all the FeP lines.
PrP-MnP	24 hrs. at $1100°$ C.	Appears to contain the PrP lines and all MnP lines.
PrP-CrP	24 hrs. at $1100°$ C.	Mixture of PrP and CrP.

Table XIIIB. Phosphorus Systems (Continued)

Reaction Attempted	Time and Temperature	Results
	YbP-MP Systems	
YbP-FeP	24 hrs. at 1100° C.	Appears to contain all YbP lines and all FeP lines.
YbP-MnP	24 hrs. at 1100° C.	Appears to contain all YbP lines and all MnP lines.
YbP-CrP	24 hrs. at 1100° C.	Appears to contain all YbP lines and all CrP lines.

V. QUATERNARY SYSTEMS

VA. Introduction

Attempts were made to synthesize compounds by solid state reaction of YbAs, YbP, and GdAs with CdI_2 in various molar ratios. There appeared to be a possibility of obtaining compounds with the spinel structure (such as $CdYb_2As_2I_2$).

Suchow and Stemple[7] reported the spinel in which the octahedral sites of spinel (discussed on page 6) were occupied by rare earth ions, e.g. CdY_2S_4, CdY_2Se_4, $CdTm_2S_4$, $CdTm_2Se_4$.

The present work was initiated in an attempt to synthesize compounds with a spinel structure, i.e. the octahedral sites occupied by ytterbium; and since in the above spinels S is a divalent anion, it is probably possible to substitute two anions with different valence states (I^- and As^{3-}) for two S^{2-} ions to obtain a new compound with the spinel structure.

Suchow et al[44] have reported zinc phosphide (Zn_3PI_3) and zinc arsenide iodide (Zn_3AsI_3) with disordered defect zincblende structure. There was another possibility in the present work to obtain mixed a iodide-arsenide (or phosphide) with similar composition, but different

structure (it is impossible to prepare a compound with this structure in which the rare earth element enters tetrahedral sites).

VB. PREPARATION

Cadmium iodide crystal of 99.5% purity was obtained from the Allied Chemical Company. YbAs and GdAs were prepared as discussed before.

Following this, attempts were made to prepare the quaternary compounds in the following manner:

1. Stoichiometric amounts of compounds were weighed.

2. Compounds were thoroughly ground together and put in a quartz reaction tube.

3. A vacuum was drawn on the tube for five minutes to remove any air which might oxidize the compounds. To insure the complete removal of air from the tube, the tube was then flushed with argon. This process was repeated three times followed by a final five minute evacuation. After this period, the tubes were sealed using an oxygen-natural gas torch.

4. The tubes were put in a muffle furnace at different temperatures for various lengths of time.

5. The tubes were cooled by quenching in cold water.

6. The compounds were ground into fine powder and analyzed by the X-ray diffraction using Norelco equipment with 57.3mm powder cameras.

VC. RESULTS AND DISCUSSION

In this system, in all cases, the X-ray powder diffraction of the products indicated no formation of compounds of the types sought, but in all cases they showed some new compounds. The results are shown in Table XIV. Some products were found separated into two parts (A & B). For all samples the B part had a yellowish green color and the A part looked like a metallic crystal. When the shiny crystal (A) was ground it was black.

It is interesting that with the same molar ratio of YbAs and CdI_2 but different temperatures, different compounds are obtained. It was found that the formation of these compounds is temperature-dependent. For both $YbAs-CdI_2$ and $2YbAs-CdI_2$ at the same temperature the same compounds were obtained.

In many cases new compounds appeared to be formed but because of the complexity of the X-ray patterns it was not possible to determine the structure of these compounds.

In the case of $CdI_2 + 2YbAs$ at $570°C$. the lines were checked against different possible structures that have been reported up to now. Asprey et al[45] have reported YbI_3 with hexagonal symmetry and lattice dimensions of a=7.434 Å, and c=20.72 Å. No data on the d-spacings of this compound were given. Since DyI_3 has the same structure

and Dy and Yb are close to each other in the periodic
table, the d-spacings and intensities for these two com-
pounds (DyI_3 & YbI_3) should be similar. By comparing
intensities of the two compounds and using the reported
hkl values and lattice constants of DyI_3, d-spacings of
YbI_3 were calculated.

Table XIV. Experimental Data of CdI_2-MAs System

	Temperature and Time	Comment on X-ray diffraction pattern	Color
		Unseparated Compounds	
CdI_2-2YbAs	24 hrs. at 570° C.	YbAs+CdI_2 + a few new lines	Yellowish-Green
CdI_2-2YbP	24 hrs. at 570° C.	YbP+CdI_2 lines	Yellowish-Green
CdI_2-2YbP	24 hrs. at 450° C.	YbP lines	Yellowish-Green
CdI_2-2YbAs	24 hrs. at 1000° C.	YbAs+As + new lines	Yellowish-Green
CdI_2-2YbP	24 hrs. at 1000° C.	YbP lines	Yellowish-Green
		B Portion of Products	
CdI_2-2YbAs	24 hrs. at 470° C.	YbAs + new lines	Yellowish-Green
CdI_2-2YbAs	24 hrs. at 720° C.	YbAs+CdI_2 lines	Yellowish-Green
CdI_2-2YbP	24 hrs. at 720° C.	YbP lines	Yellowish-Green
CdI_2-2YbAs	24 hrs. at 570° C.	YbAs+YbI_3 lines	Yellowish-Green
YbAs-CdI_2	24 hrs. at 570° C.	YbAs+YbI_3 lines	Yellowish-Green
GdAs-CdI_2	24 hrs. at 570° C.	GdAs + new lines	Yellowish-Green

Table XIV. Experimental Data of CdI_2-MAs System (Continued)

	Temperature and Time	Comment on X-ray diffraction pattern	Color
	A Portion of Products (Shiny Part)		
CdI_2-2YbAs	24 hrs. at 470° C.	YbAs + many new lines	Black
CdI_2-2YbAs	24 hrs. at 720° C.	YbAs+Cd_3As_2 lines	Black
CdI_2-2YbP	24 hrs. at 720° C.	CdI_2 + new lines	Black
CdI_2-2YbAs	24 hrs. at 570° C.	YbAs + new lines	Black
YbAs-CdI_2	24 hrs. at 570° C.	YbAs+Cd_3As_2 lines	Black
YbAs-2CdI_2	24 hrs. at 570° C.	New lines	Black
GdAs-CdI_2	24 hrs. at 520° C.	GdAs + many new lines	Black

The d-spacings calculated were the same as observed d-spacings of the present sample proving the present sample was YbI_3. The data is shown in Table XV.

Table XV. X-ray Diffraction Patterns of DyI_3 and YbI_3[45]

DyI_3 Hexagonal a=7.488Å, c=20.833Å			YbI_3 Hexagonal a=7.434Å, c=20.72Å		Product of $CdI_2+2YbAs$ (at 570°C) (B-Portion)		
d(Å)	I	(hkl)	d(calc.) (Å)	(hkl)	d(obs.) (Å)	I(obs.)*	Comment
3.30	10	113	3.280	113	3.28	vs	YbI_3 line
-	-	-	-	-	2.83	vs	YbAs line
2.54	8	116	2.53	116	2.53	s+	YbI_3 line
2.31	1	122	2.37	112	2.37	vw	YbI_3 line
2.165	6	300	2.146	300	2.15	s	YbI_3 line
2.068	2	303	2.05	303	2.00	vw	YbI_3 line
1.968	9	119	1.96	119	1.96	w	YbI_3 line
1.837	3	306	1.82	306	1.82	vw	YbI_3 line
-	-	-	-	-	1.71	vs	YbAs line

*In the pattern the YbI_3 lines are not the strongest ones and this intensity shows the strength of YbI_3 lines compared with each other.

Table XV.   X-ray Diffraction Patterns of DyI_3 and YbI_3 (Continued)

DyI_3-Hexagonal a=7.488Å, c=20.833Å			YbI_3-Hexagonal a=7.434Å, c=20.72Å		Product of CdI_2-2YbAs (at 570°C) (B-Portion)		
d(Å)	I	(hkl)	d(calc.) (Å)	(hkl)	d(obs.) (Å)	I(obs.)*	Comment
1.651	4	226	1.636	226	1.64	w	YbI_3 line
-	-	-	-	-	1.42	s	YbAs line
1.355	5	30.12	1.345	30.12	1.35	w	YbI_3 line
-	-	-	-	-	1.30	w	YbAs line

*In the pattern, the YbI_3 lines are not the strongest ones and this intensity shows the strength of YbI_3 lines compared with each other.

By comparing data reported by Passerini[46] for Cd_3As_2 with one of the separated products of reaction between YbAs-CdI_2 at 570° C. and reaction between CdI_2+2YbAs at 720° C. it was found that they contain Cd_3As_2. It therefore appears that CdI_2 and YbAs reacted to form Cd_3As_2 and YbI_3.

Cd_3As_2 is tetragonal with a unit containing eight molecules and having the cell dimensions:

$$a=8.945 \text{ Å.} \qquad c=12.65 \text{ Å.}$$

Data reported by Passerini[46] is given in Table XVI and this data compared with those for the present sample.

Table XVI. X-ray Diffraction Pattern of Cd_3As_2.

Cd_3As_2-Hexagonal (ref. no. 46)			Product of CdI_2+YbAs and CdI_2+2YbAs (A Portion)		
hkl	d, Å.	Intensity	d,Å.	Intensity*	Comment
–	–	–	2.83	s	YbAs-line
210	2.81	60	2.80	s	Cd_3As_2 line
220	2.22	100	2.22	vs	Cd_3As_2 line
–	–	–	2.00	s	YbAs line
311	1.90	60	1.90	s	Cd_3As_2 line
222	1.81	50	1.80	s–	Cd_3As_2 line
–	–	–	1.71	w	YbAs line
422	1.28	90	1.28	s	Cd_3As_2 line
440	1.11	90	1.11	s–	Cd_3As_2 line

*Intensity abbreviation: s, strong; w, weak; vs, very strong.

VI.   TERNARY SYSTEMS

Attempts were made to prepare ternary compounds in the systems YbI_3-YbAs and GdI_2-GdAs. It was hoped to obtain a simple phase which might help to interpret the quaternary system discussed in section V.

Preparation

Gadolinium iodide and ytterbium iodide of 99.99% purity were obtained from the American Potash & Chemical Corporation. YbAs and GdAs were prepared as discussed before.

Following this, the ternary compounds were prepared in the following manner:

1.   Stoichiometric amounts of compounds were weighed.

2.   Compounds were thoroughly ground together under dry nitrogen and put in a quartz reaction tube.

3.   A vacuum was drawn on the tube for five minutes to remove any air which might oxidize the compounds. To insure the complete removal of air from the tube, the tube was then flushed with argon. This process was repeated three times followed by a final five minutes evacuation. After this period, the tubes were sealed using an oxygen-natural gas torch.

4.   The tubes were put in a muffle furnace at 570° C. for 24 hours.

5. The tubes were cooled by quenching in cold water.

6. Compounds were ground into fine powder (in the case of GdI_2-GdAs it was possible to separate the compound into two parts) and analyzed by the X-ray diffraction method using Norelco equipment with 57.3-mm powder cameras.

VIB. RESULTS

Although new X-ray lines indicating a new compound were found, it was so complicated that determination of crystal parameters was impossible.

1. In the case of YbI_3_YbAs, it was found that the product contained YbI_3 and YbAs phases and also a few new lines. The product was greenish-yellow and it picked up water.

2. In the case of GdI_3_GdAs the product was greenish-yellow and it was possible to separate it into two parts, greenish-yellow and shiny crystals. The shiny part of this product was As, and the greenish-yellow part contained GdI_3 and GdAs lines plus a few new lines.

VII.   THE REFLECTANCE OF Pr AND Nd GARNETS

VIIA.   Introduction[47,48]

The electrons responsible for the spectral properties of lanthanide ions are 4f electrons, and the 4f orbitals are very effectively shielded from interaction with external forces by the overlying $6s^2$ and $6p^2$ shells. Hence the states arising from the various $4f^n$ configurations are only slightly affected by the surrounding of the ions and remain partically unvariant for a given ion in all of its compounds.

Because the f orbitals are so well shielded from the surrounding of the ions, the various states arising from the f^n configurations are split by external fields only to the extent of ~ 100 cm^{-1}. Thus when electronic transitions, called f-f transitions, occur from one J state of an f^n configuration to another J state of this configuration, the absorption bands are extremely sharp. Virtually all of the absorption bands found in the visible and near-ultraviolet spectra of the lanthanide ions have this line-like character. There are, however, bands found in some cases which are quite broad; these may be assigned to transitions in which an f electron is excited to an outer d, s, or p orbital. Barnes[49] has reported that there are also some broad bands due to

ligand-to-metal charge transfer with reducing ligands. The color and electronic ground state of the tripositive ions are given in Table XVII.

When a rare earth ion is placed in a crystal lattice, it is subject to a number of forces which are absent in the free ion. There are, for instance, resonance interactions with neighboring ions of the same kind, and there are electric and magnetic interactions with each individual ion in the vicinity. Some of these interactions may represent a coupling to the crystal lattice, so that the rare earth ion can transfer some or all of its energy to crystal lattice vibrations.

GARNETS

Garnets are of interest largely because of their useful magnetic and optical properties. An example of a ferrimagnetic garnet is yttrium iron garnet, $\{Y_3\}$ $[Fe_2]$ $(Fe_3)O_{12}$, (where the curly brackets indicate eightfold dodecahedral coordination, the square brackets sixfold octahedral coordination, and the parentheses fourfold tetrahedral coordination). Two other kinds of garnets, yttrium aluminum garnet (YAG), and yttrium gallium garnet (YGG) are transparent in the near infrared. Garnets have also been prepared with rare earths in place of yttrium). The yttrium gallium garnets and the yttrium aluminum garnets have quite

Table XVII. Color and Electric Ground States of the M^{3+} Ions. From Cotton and Wilkinson, <u>Advanced Inorganic Chemistry</u> 3rd Edition, Interscience Publishers, 1966, p. 1056.

Ion	Ground State	Color
La	$^1S_0$	Colorless
Ce	$^2F_{5/2}$	Colorless
Pr	$^3H_4$	Green
Nd	$^4I_{9/2}$	Reddish
Pm	$^5I_4$	Pink; Yellow
Sm	$^6H_{5/2}$	Yellow
Eu	$^7F_0$	Pale Pink
Gd	$^8S_{7/2}$	Colorless
Tb	$^7F_6$	Pale Pink
Dy	$^6H_{15/2}$	Yellow
Ho	$^5I_8$	Pink Yellow
Er	$^4I_{15/2}$	Reddish
Tm	$^3H_6$	Green
Yb	$^2F_{7/2}$	Colorless
Lu	$^1S_0$	Colorless

different crystal fields. It appears that all rare-earth ions placed into either of the garnets show distinct though relatively weak fluorescence. There are a great variety of other artificially produced garnets, on most of which the optical studies have not yet been reported.

The present work was initiated to study the reflectance spectra of praseodymium and neodymium garnets with rare-earths on two crystallographic sites which had been prepared in this laboratory[3]. There had been observed color differences in some of these garnets with varying quantities of rare earths on two crystallographic sites, e.g. $\{Pr_{2.5}Yb_{0.5}\}$ $[Ga_2]$ $(Ga_3)O_{12}$, $\{Pr_{2.5}Yb_{0.5}\}$ $[YbGa]$ $(Ga_3)O_{12}$, $\{Pr_{2.5}Yb_{0.5}\}$ $[Yb_{1.5}Ga_{0.5}]$ $(Ga_3)O_{12}$, and $\{Pr_{2.5}Yb_{0.5}\}$ $[Yb_2]$ $(Ga_3)O_{12}$, have somewhat different colors. Attempts were made to compare the reflectance of garnets with reference garnets with the same rare earth ions on one of the sites, e.g. comparison of the above garnets with $\{Pr_3\}$ $[Ga_2]$ $(Ga_3 O_{12}$ (with Pr in the dodecahedral site), $\{Yb_3\}$ $[Ga_2]$ $(Ga_3)O_{12}$, (with Yb in the dodecahedral site), and $\{Sr_3\}$ $[Yb_2]$ $(Ge_3)O_{12}$, (with Yb in the octahedral site). Table XVIII shows the garnets studied in the present work. The instrument employed was not suitable for measuring line spectra, and only band spectra was measured.

Table XVIII. Classification of Garnets.

Compound	Color
A. Nd-Tm Class	
1. $\{Nd_3\}\ [Ga_2]\ (Ga_3)O_{12}$	Lavender
2. $\{Tm_3\}\ [Ga_2]\ (Ga_3)O_{12}$	White (perhaps a little off color)
3. $\{Sr_3\}\ [Tm_2]\ (Ge_3)O_{12}$	Tannish white
4. $\{Nd_{2.4}Tm_{0.6}\}\ [Tm_2]\ (Ga_3)O_{12}$	Lavender
5. $\{Nd_{2.4}Tm_{0.6}\}\ [Tm_{1.6}Ga_{0.4}]\ (Ga_3)O_{12}$	Lavender
6. $\{Nd_{2.4}Tm_{0.6}\}\ [Tm_{0.8}Ga_{1.2}]\ (Ga_3)O_{12}$	Lavender
7. $\{Nd_{2.4}Tm_{0.6}\}\ [Ga_2]\ (Ga_3)O_{12}$	Lavender
B. Nd-Er Class	
1. $\{Nd_3\}\ [Ga_2]\ (Ga_3)O_{12}$	Lavender
2. $\{Er_3\}\ [Ga_2]\ (Ga_3)O_{12}$	Lavender
3. $\{Sr_3\}\ [Er_2]\ (Ge_3)O_{12}$	Lavender
4. $\{Nd_{1.9}Er_{1.1}\}\ [Er_{1.5}Ga_{0.5}]\ (Ga_3)O_{12}$	Lavender
5. $\{Nd_{1.9}Er_{1.1}\}\ [Ga_2]\ (Ga_3)O_{12}$	Lavender
C. Nd-Yb Class	
1. $\{Nd_3\}\ [Ga_2]\ (Ga_3)O_{12}$	Lavender
2. $\{Yb_3\}\ [Ga_2]\ (Ga_3)O_{12}$	White
3. $\{Sr_3\}\ [Yb_2]\ (Ge_3)O_{12}$	White
4. $\{Nd_{2.7}Yb_{0.3}\}\ [Yb_2]\ (Ga_3)O_{12}$	Lavender
5. $\{Nd_{2.7}Yb_{0.3}\}\ [Yb_{1.5}Ga_{0.5}]\ (Ga_3)O_{12}$	Lavender
6. $\{Nd_{2.7}Yb_{0.3}\}\ [Ga_2]\ (Ga_3)O_{12}$	Lavender

Table XVIII.   Classification of Garnets (Continued)

Compound	Color

D.   Pr-Tm Class

1. $\{Pr_3\}$ $[Ga_2]$ $(Ga_3)O_{12}$	Greenish-Yellow
2. $\{Tm_3\}$ $[Ga_2]$ $(Ga_3)O_{12}$	White (perhaps a little off color)
3. $\{Sr_3\}$ $[Tm_2]$ $(Ge_3)O_{12}$	Tannish white
4. $\{Pr_{2.2}Tm_{0.8}\}$ $[Tm_2]$ $(Ga_3)O_{12}$	Yellow with a slightly greenish tint
5. $\{Pr_{2.2}Tm_{0.8}\}$ $[Tm_{1.5}Ga_{0.5}]$ $(Ga_3)O_{12}$	Greenish-Yellow
6. $\{Pr_{2.2}Tm_{0.8}\}$ $[TmGa]$ $(Ga_3)O_{12}$	Greenish-Yellow
7. $\{Pr_{2.2}Tm_{0.8}\}$ $[Ga_2]$ $(Ga_3)O_{12}$	Greenish-Yellow

E.   Pr-Er Class

1. $\{Pr_3\}$ $[Ga_2]$ $(Ga_3)O_{12}$	Greenish-Yellow
2. $\{Er_3\}$ $[Ga_2]$ $(Ga_3)O_{12}$	Lavender
3. $\{Sr_3\}$ $[Er_2]$ $(Ge_3)O_{12}$	Lavender
4. $\{Pr_{1.85}Er_{1.15}\}$ $[Er_{1.75}Ga_{0.25}]$ $(Ga_3)O_{12}$	Dull Yellow
5. $\{Pr_{1.85}Er_{1.15}\}$ $[Ga_2]$ $(Ga_3)O_{12}$	Dull Yellow

F.   Pr-Yb Class

1. $\{Pr_3\}$ $[Ga_2]$ $(Ga_3)O_{12}$	Greenish-Yellow
2. $\{Yb_3\}$ $[Ga_2]$ $(Ga_3)O_{12}$	White
3. $\{Sr_3\}$ $[Yb_2]$ $(Ge_3)O_{12}$	White
4. $\{Pr_{2.5}Yb_{0.5}\}$ $[Yb_2]$ $(Ga_3)O_{12}$	Dark Tan
5. $\{Pr_{2.5}Yb_{0.5}\}$ $[Yb_{1.5}Ga_{0.5}]$ $(Ga_3)O_{12}$	Yellowish-Tan
6. $\{Pr_{2.5}Yb_{0.5}\}$ $[YbGa]$ $(Ga_3)O_{12}$	Dull Yellow
7. $\{Pr_{2.5}Yb_{0.5}\}$ $[Ga_2]$ $(Ga_3)O_{12}$	Yellow

VIIB. <u>EXPERIMENTS</u>

The equipment used in this investigation was the Beckman Model DU spectrophotometer. Wavelengths employed were from 350-750 mμ, and the slit width 0.3-0.9 millimeters.

The Beckman DU spectrophotometer[50] is a single-beam, non-recording instrument for the ultraviolet and visible regions. For the ultraviolet region, a hydrogen discharge lamp with a very thin glass window serves as the source and for the visible region operation it has a tungsten lamp. The optical system is shown in Fig. 2. S is the source of light. Radiation from the source, S, is reflected by a small mirror in the source housing onto the plane mirror next to the slit and it is thus reflected into the monochromator. A spherical mirror collimates the beam and sends it into the quartz Littrow prism. The beam returns along virtually the same path, passing out the same slit, and then through the sample (or reference) compartment and onto the detector P. The detector is either a red-sensitive (above 625 mμ) phototube or blue-sensitive (below 625 mμ) photomultiplier.

The frequency range passing through the sample is controlled by rotating the prism by means of a rod passing through the top of the case. The transmittance

of a sample is determined by adjusting the instrument
to read 100% T with a reference cell in place, then
rebalancing the instrument with the sample in place by
turning the knob attached to the potentiometer and the
transmittance scale.

For reflectance studies the reflectance attachment
was used and it is shown in Fig. 3. Monochromatic radi-
ation from slit D is made less divergent by quartz lens
L, which after reflection from the front-surface plane
mirror, M, irradiates the sample S. A portion of the
diffuse reflected light from the sample, is reflected
from the ellipsoidal metal mirror R onto the diffusing
envelope, H, of a phototube and then to the photosensitive
surface. The hollow cone of light includes an angle of
approximately $20°$ about the line SR. Thus, light rays
from the center of the sample surface (or reference)
making angles of $35°$ to $55°$ with the perpendicular are
measured.

The sample and reference materials are placed in a
sliding drawer located at the bottom of the accessory.
Because the samples available were small, a smaller
than usual surface was used and the rest of the surface
of the sample holder was painted black. Since the sur-
face area of sample and reference should be equal, a
hole as big as the surface of the sample was cut in
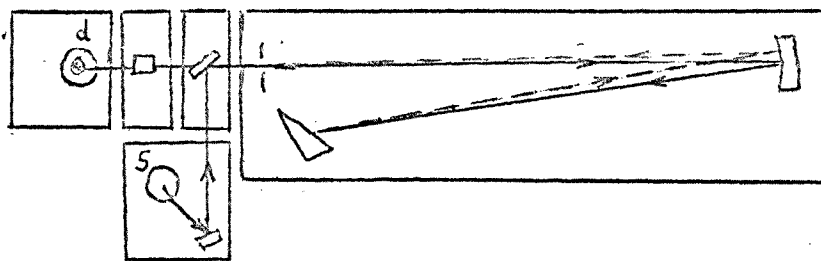
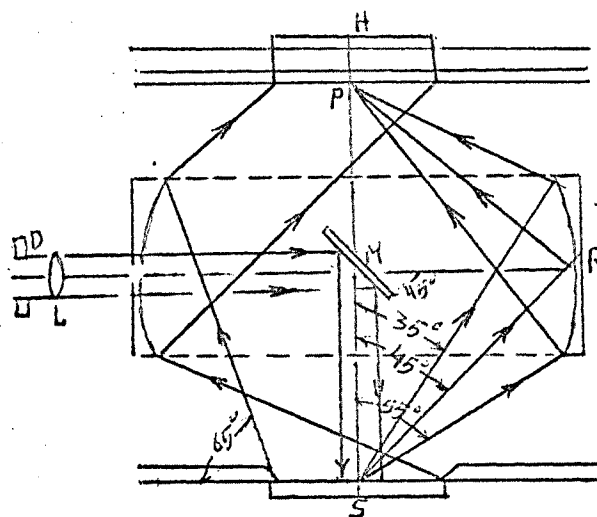Fig. 2. Beckman DU spectrophotometer for ultraviolet and visible regions.

Fig. 3. Schematic cross section of reflectance attachment showing geometry of irradiation and reception. D, slit; L, lens; M, mirror; S, specimen; R, ellipsoidal reflector; P, diffusing quartz plate; H, phototube envelope.

black paper and it was put on the surface of the reference
(a block of magnesium carbonate).

The reflectance of samples were determined by ad-
justing the instrument to read 100% reflectance with the
reference (block of magnesium carbonate) cell in place,
then rebalancing the instrument with the sample in place
(by pushing the drawer into the reflectance attachment)
by turning the knob attached to the potentiometer and the
reflectance scale.

The reflectance percent of samples for different
wavelengths (from 350-750 mμ) were measured. The values
of reflectance percents that were read from instrument
were corrected by using the coefficients of reflection
of $MgCO_3$ reported by Benford and Schwarz[49].

The corrected percent reflectance was plotted
against wavelength. In order to make it easier to com-
pare the samples, they were classified as in Table XVII,
and all samples in each class were plotted together
(Fig. 4 to Fig. 9).

VIIC. RESULTS AND DISCUSSION

The experimental results are given in terms of percent reflectance vs wavelength ($m\mu$) in Figs. 4 to 9. The samples were classified in six classes (Table XVIII).

A. Nd-Tm Class

The experimental result of this class is given in Fig. 4. Since $\{Nd_3\}\,[Ga_2]\,(Ga_3)O_{12}$ has Nd on the dodecahedral site, $\{Tm_3\}\,[Ga_2]\,(Ga_3)O_{12}$ has Tm on the dodecahedral site, and $\{Sr_3\}\,[Tm_2]\,(Ge_3)O_{12}$ has Tm on the octahedral sites, these three garnets were taken as reference. Four garnets, $\{Nd_{2.4}Tm_{0.6}\}\,[Tm_2]\,(Ga_3)O_{12}$, $\{Nd_{2.4}Tm_{0.6}\}\,[Tm_{1.6}Ga_{0.4}]\,(Ga_3)O_{12}$, $\{Nd_{2.4}Tm_{0.6}\}\,[Tm_{0.8}Ga_{1.2}]\,(Ga_3)O_{12}$, and $\{Nd_{2.4}Tm_{0.6}\}\,[Ga_2]\,(Ga_3)O_{12}$, with different atomic ratios of Tm on both crystallographic sites were studied and their reflectance spectra were compared with the three above references. The spectral bands of these four garnets were nearly identical with those of the references. Therefore, no interaction between rare earth ions was observed.

B. Nd-Er Class

Since the color of all garnets in this class is the same (lavender) it was expected that there would be no extra absorption when comparing the spectral bands of garnets (with different atomic ratios of Er on both

crystallographic sites) with the references $\{Nd_3\}$ $[Ga_2]$ $(Ga_3)O_{12}$, $\{Er_3\}$ $[Ga_2]$ $(Ga_3)O_{12}$, and $\{Sr_3\}$ $[Er_2]$ $(Ge_3)O_{12}$. The experimental results of this class are given in terms of percent reflectance vs wavelength $(m\mu)$ in Fig. 5. The spectral bands of the $\{Nd_{1.9}Er_{1.1}\}$ $[Er_{1.5}Gd_{0.5}]$ $(Ga_3)O_{12}$, and $\{Nd_{1.9}Er_{1.1}\}$ $[Ga_2]$ $(Ga_3)O_{12}$ were identical with those of the references.

C. Nd-Yb Class

The experimental results of this class are given in terms of percent reflectance vs wavelength $(m\mu)$ in Fig. 6. $\{Nd_3\}$ $[Ga_2]$ $(Ga_3)O_{12}$, $\{Yb_3\}$ $[Ga_2]$ $(Ga_3)O_{12}$, and $\{Sr_3\}$ $[Yb_2]$ $(Ge_3)O_{12}$ were taken as references and the reflectance spectra of $\{Nd_{2.7}Yb_{0.3}\}$ $[Yb_2]$ $(Ga_3)O_{12}$, $\{Nd_{2.7}Yb_{0.3}\}$ $[Ga_2]$ $(Ga_3)O_{12}$, and $\{Nd_{2.7}Yb_{0.3}\}$ $[Yb_{1.5}Ga_{0.5}]$ $(Ga_3)O_{12}$ with different atomic ratios of Yb on both crystallographic sites were compared with those of the references. The spectral bands of three last garnets were identical with those of the references and no extra absorption was seen.

D. Pr-Tm Class

In this class, $\{Pr_3\}$ $[Ga_2]$ $(Ga_3)O_{12}$, $\{Tm_3\}$ $[Ga_2]$ $(Ga_3)O_{12}$, and $\{Sr_3\}$ $[Tm_2]$ $(Ge_3)O_{12}$ were taken as references and the reflectance spectra of $\{Pr_{2.2}Tm_{0.8}\}$ $[Tm_2]$ $(Ga_3)O_{12}$, $\{Pr_{2.2}Tm_{0.8}\}$ $[Tm_{1.5}Ga_{0.5}]$ $(Ga_3)O_{12}$, $\{Pr_{2.2}Tm_{0.8}\}$ $[TmGa]$

$\cdot (Ga_3)O_{12}$, and $\{Pr_{2.2}Tm_{0.8}\}$ $[Ga_2](Ga_3)O_{12}$ were compared with those of the references. The experimental results are given in Fig. 7. The spectral bands of these four last garnets were nearly identical with those of the references.

E. Pr-Er Class

The experimental results of this class are given in terms of percent reflectance vs wavelength (mμ) in Fig. 8. The spectral bands of $\{Pr_{1.85}Er_{1.15}\}$ $[Er_{1.75}Ga_{025}]$ $(Ga_3)O_{12}$ and $\{Pr_{1.85}Er_{1.15}\}$ $[Ga_2](Ga_3)O_{12}$, are identical with those of the references, $\{Pr_3\}$ $[Ga_2](Ga_3)O_{12}$, $\{Er_3\}$ $[Ga_2](Ga_3)O_{12}$, and $\{Sr_3\}$ $[Er_2](Ge_3)O_{12}$.

F. Pr-Yb Class

The experimental results of this class are given in terms of percent reflectance vs wavelength (mμ) in Fig. 9. $\{Pr_3\}$ $[Ga_2](Ga_3)O_{12}$ (greenish-yellow), $\{Yb_3\}$ $[Ga_2](Ga_3)O_{12}$ (white), and $\{Sr_3\}$ $[Yb_2](Ge_3)O_{12}$ (white), were taken as references and reflectance spectra of $\{Pr_{2.5}Yb_{0.5}\}$ $[Yb_2](Ga_3)O_{12}$(dark tan), $\{Pr_{2.5}Yb_{0.5}\}$ $[Yb_{1.5}Ga_{0.5}]$ $(Ga_3)O_{12}$ (yellowish-tan), $\{Pr_{2.5}Yb_{0.5}\}$ $[YbGa]$ $(Ga_3)O_{12}$ (dull yellow), and $\{Pr_{2.5}Yb_{0.5}\}$ $[Ga_2]$ $(Ga_3)O_{12}$ (yellow) were compared with those of the references.

The spectral bands of $\{Pr_{2.5}Yb_{0.5}\}$ $[Ga_2](Ga_3)O_{12}$

without Yb on octahedral site are nearly identical with those of the references (shown by o in Fig. 9). In the case of the three other garnets with Yb on both crystallographic sites, their spectral bands are not identical with the spectral bands of the references. At a wavelength of 450 mμ the spectral bands of $\{Pr_{2.5}Yb_{0.5}\}$ $[YbGa]$ $(Ga_3)O_{12}$ (shown by ▲ in Fig. 9), $\{Pr_{2.5}Yb_{0.5}\}$ $[Yb_{1.5}Ga_{0.5}](Ga_3)O_{12}$ (shown by ↑ in Fig. 9), and $\{Pr_{2.5}Yb_{0.5}\}$ $[Yb_2](Ga_3)O_{12}$ (shown by □ in Fig. 9) are nearly identical with those of the references but there is more absorbance for these three garnets with Yb on both sites than those of references at wavelength of 550 mμ and around 425 mμ. The region of new absorption in terms of bands are 350-450 mμ and 490-575 mμ. Because the samples were small, the data are only semi-quantitative. The experimental results are in agreement with the colors of these garnets.

The new absorption bands are believed to be due to the presence of small quantities of Pr^{4+} and Yb^{2+} ions formed by the redox reaction $Pr^{3+} + Yb^{3+} \rightleftharpoons Pr^{4+} + Yb^{2+}$.

○ $Nd_3Ga_5O_{12}$
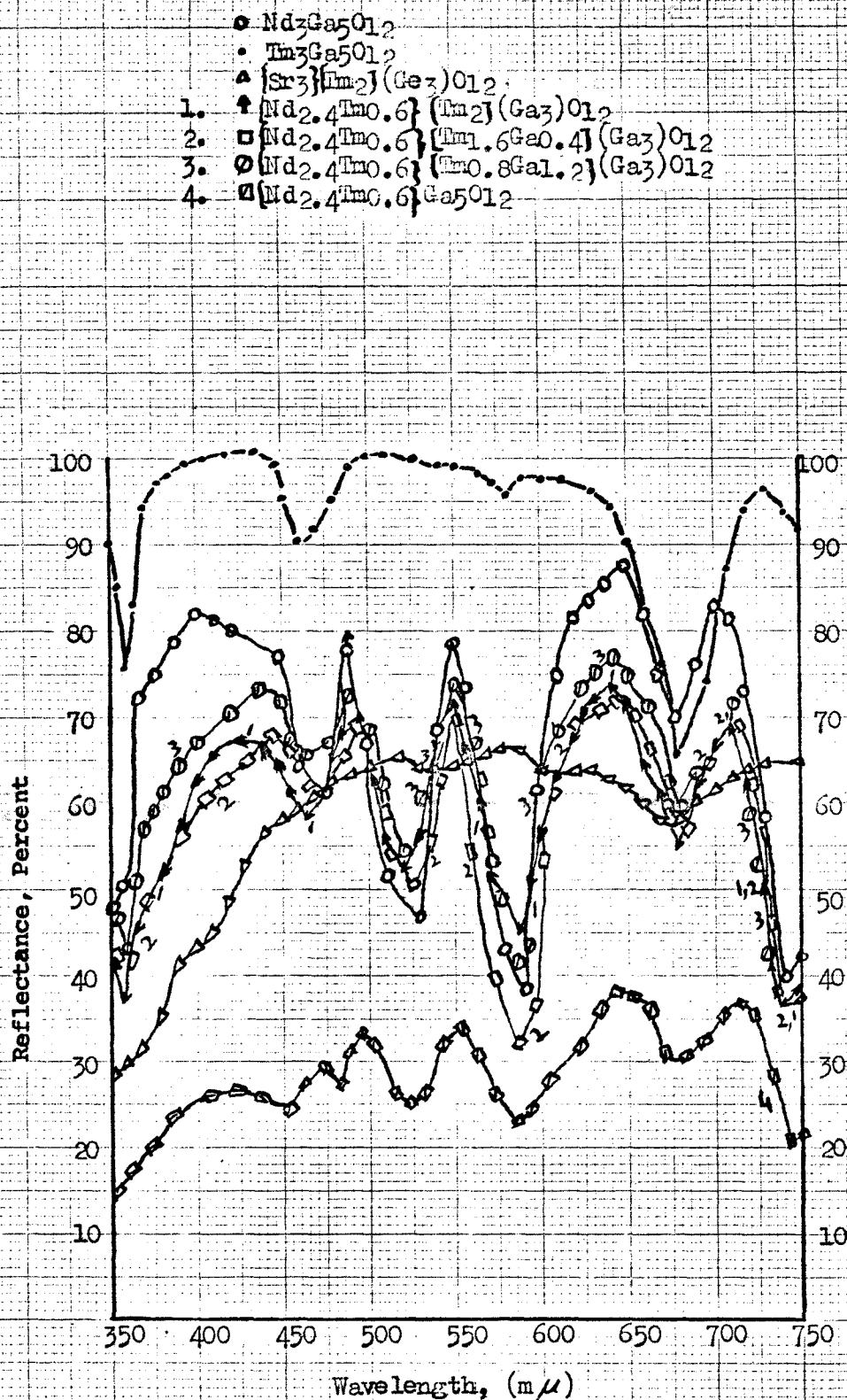● $Tm_3Ga_5O_{12}$
▲ ${Sr_3}{Tm_2}(Ge_3)O_{12}$
1. ↑ $Nd_{2.4}Tm_{0.6}{Tm_2}(Ga_3)O_{12}$
2. ▢ $Nd_{2.4}Tm_{0.6}{Tm_{1.6}Ga_{0.4}}(Ga_3)O_{12}$
3. ⌀ $Nd_{2.4}Tm_{0.6}{Tm_{0.8}Ga_{1.2}}(Ga_3)O_{12}$
4. ▨ $Nd_{2.4}Tm_{0.6}Ga_5O_{12}$

Reflectance, Percent

Wavelength, (mμ)

Fig. 4. Reflectance Spectra of Nd-Tm

Class Garnets
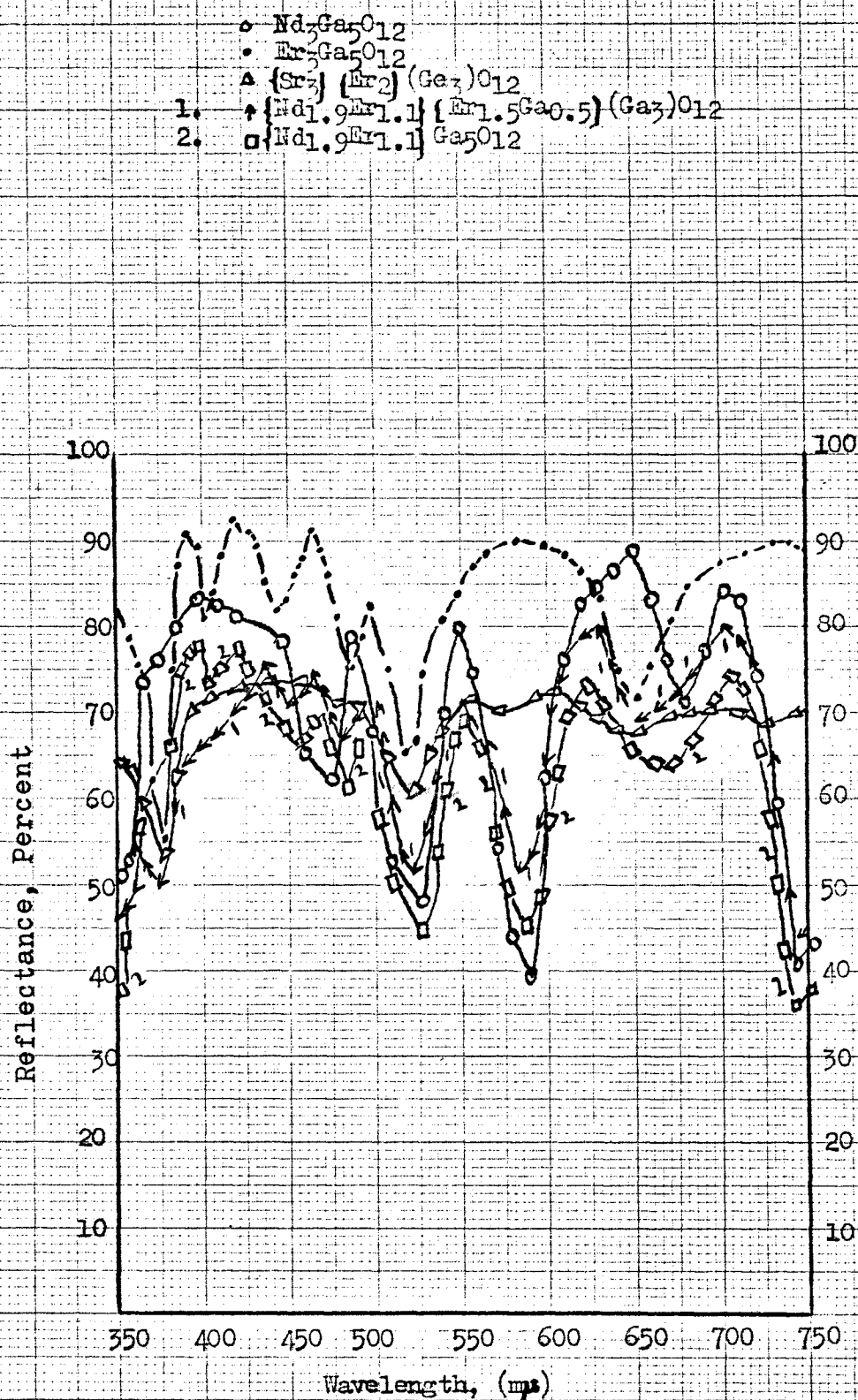
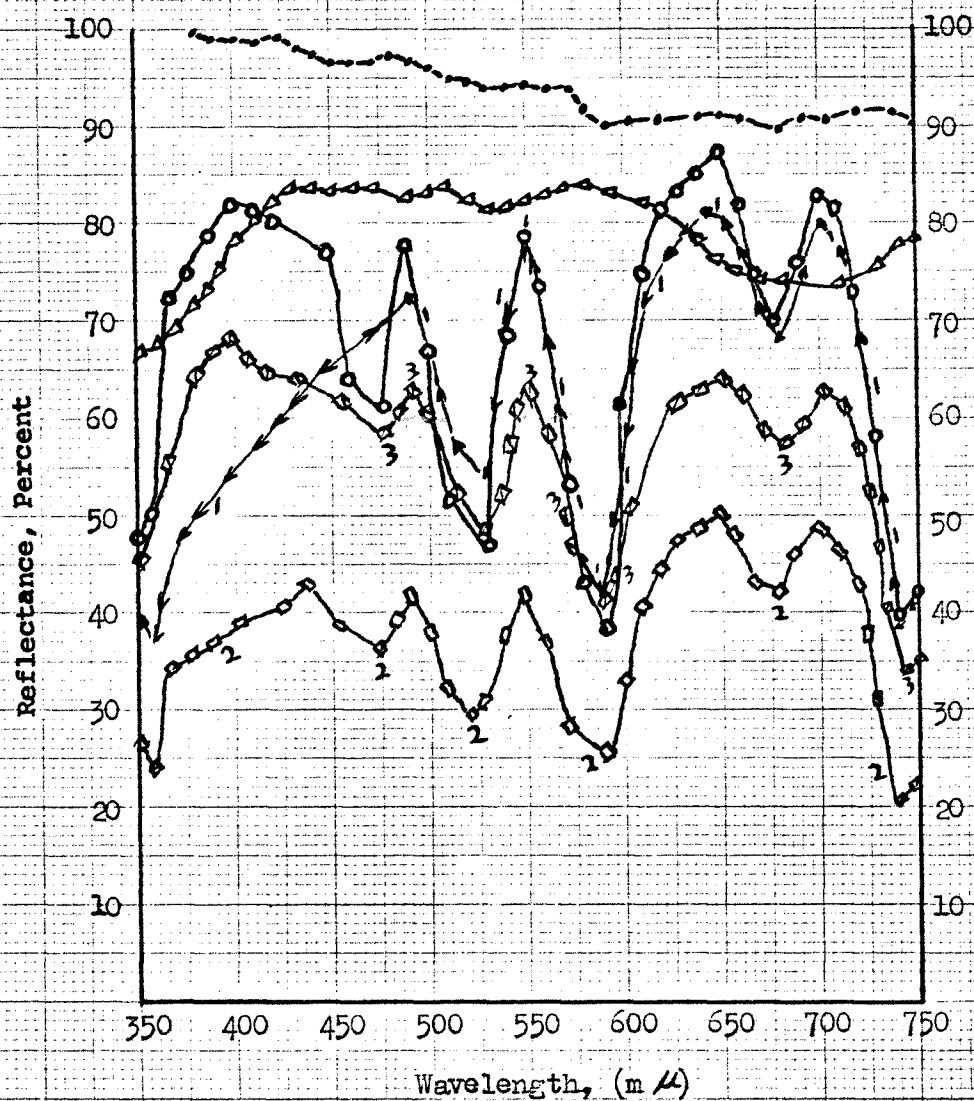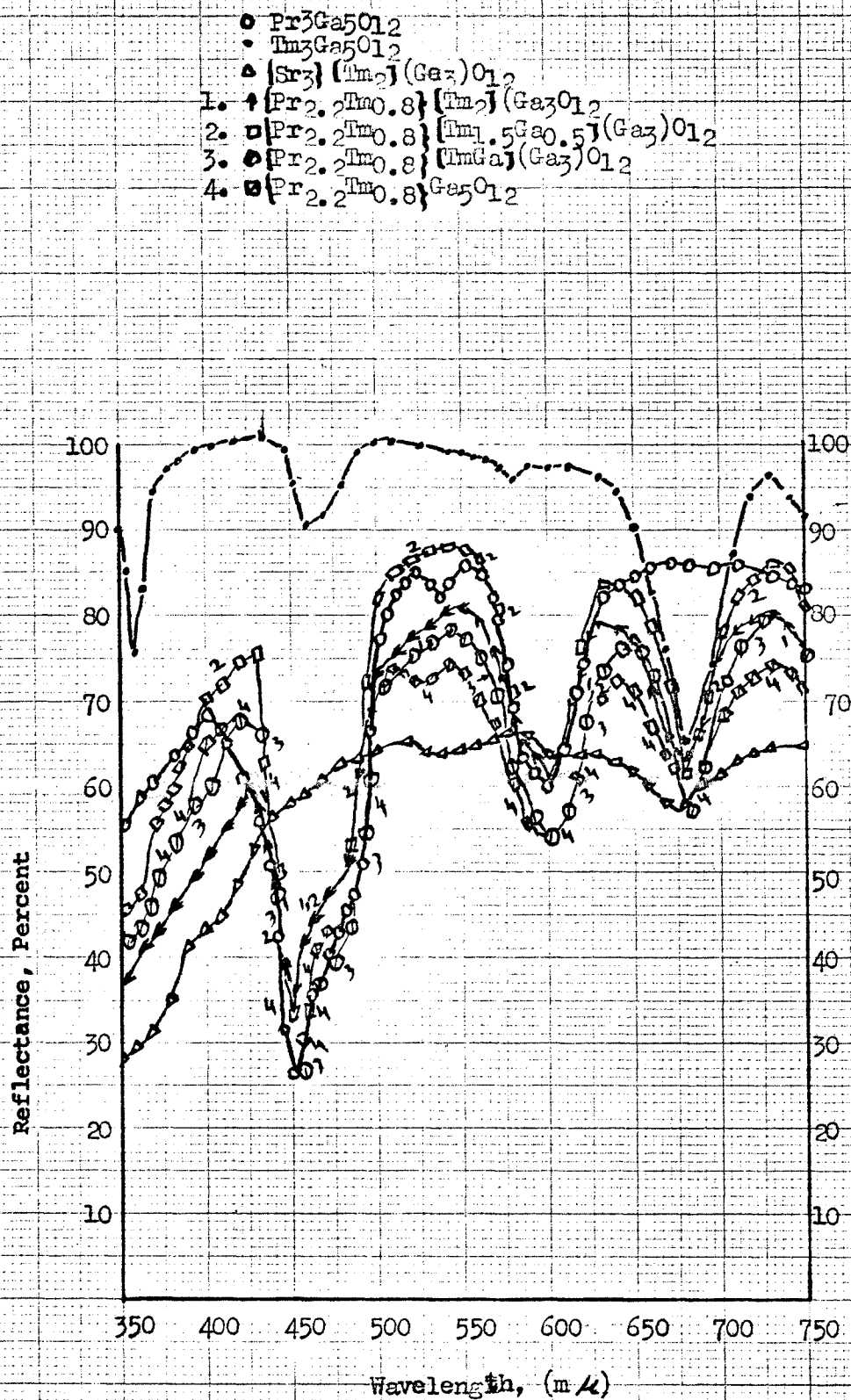Fig. 5.   Reflectance Spectra of Nd-Er

Class Garnets

Fig. 6. Reflectance Spectra of Nd-Yb

Class Garnets

Fig. 7.   Reflectance Spectra of Pr-Tm

Class Garnets
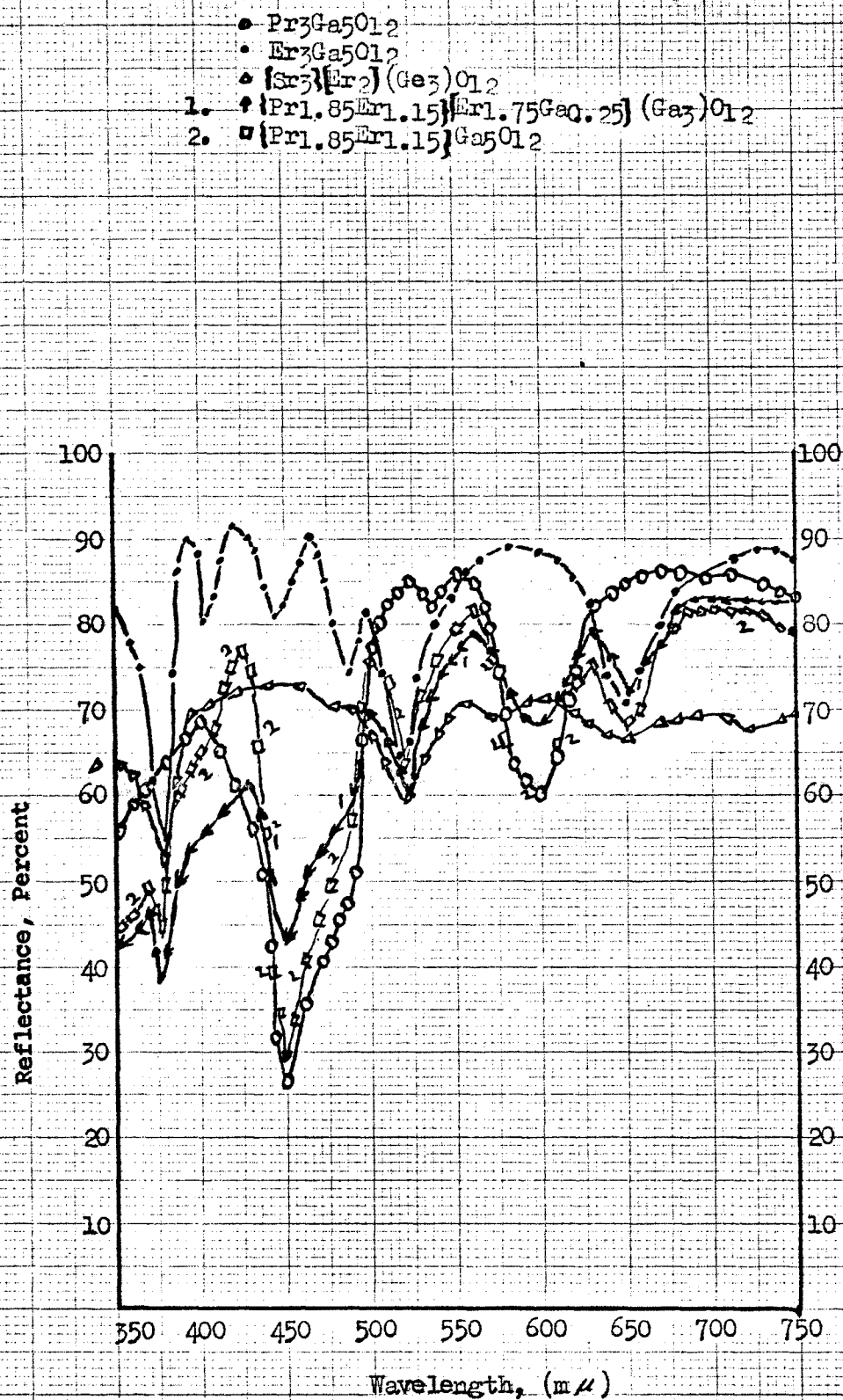
Fig. 8. Reflectance Spectra of Pr-Er

Class Garnets

Pr₃Ga₅O₁₂ and related legend:

○ $Pr_3Ga_5O_{12}$
● $Yb_3Ga_5O_{12}$
△ ${Sr_3}[Yb_2](Ge_3)O_{12}$
1. ▲ ${Pr_{2.5}Yb_{0.5}}[YbGa](Ga_3)O_{12}$
2. ♠ ${Pr_{2.5}Yb_{0.5}}[Yb_{1.5}Ga_{0.5}](Ga_3)O_{12}$
3. ▨ ${Pr_{2.5}Yb_{0.5}}Ga_5O_{12}$
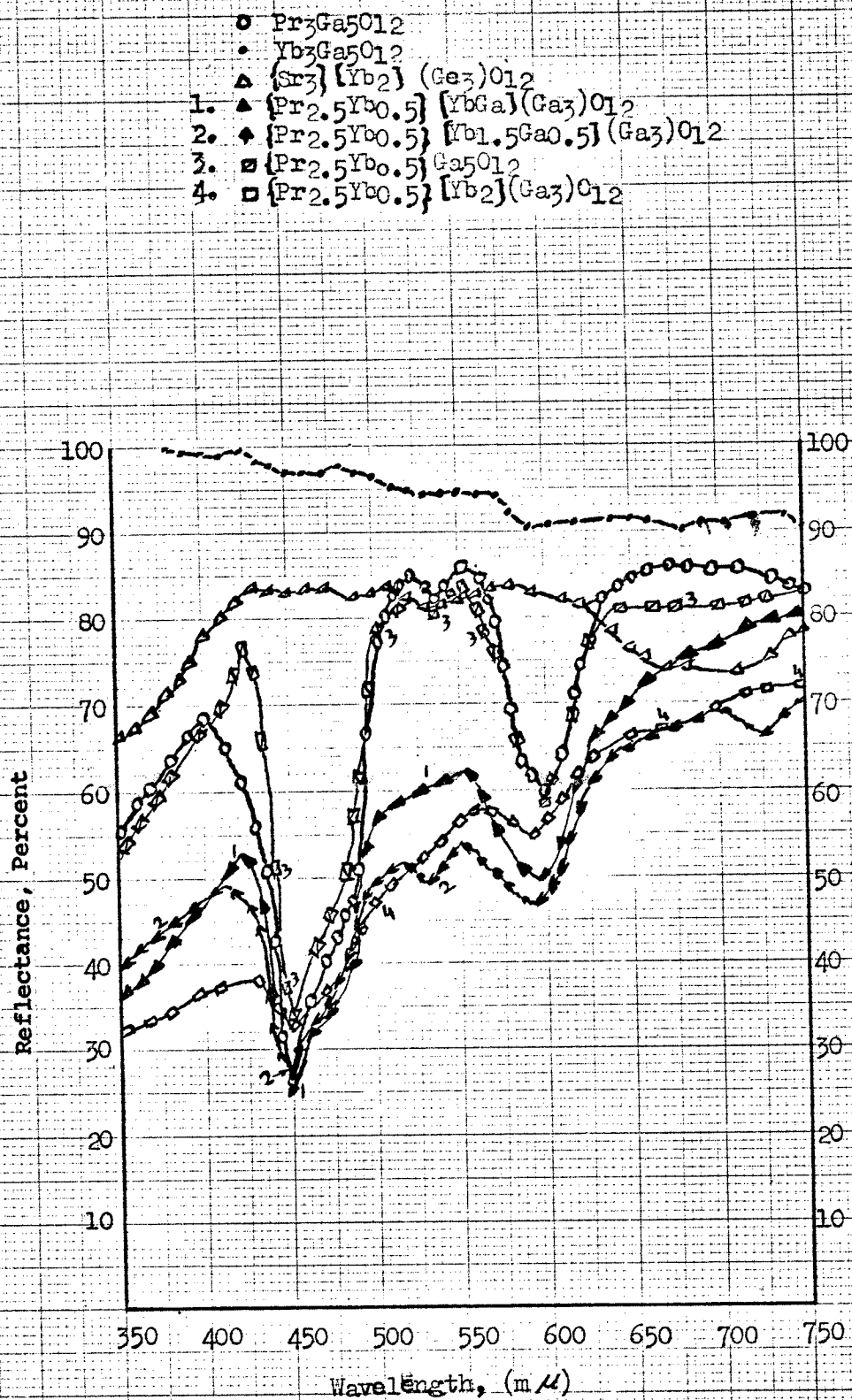4. □ ${Pr_{2.5}Yb_{0.5}}[Yb_2](Ga_3)O_{12}$

Fig. 9.   Reflectance Spectra of Pr-Yb

Class Garnets

LIST OF REFERENCES

1. Suchow, L. (private communication); Chemistry Department, Newark College of Engineering, Newark, N.J.

2. Ono, S. Despault, J. G., Calvert, L. D., and Taylor, J. B., J. Less-Common Metals, 22, 51-59 (1970).

3. Suchow, L., Kokta, M. and Flynn, V. J., J. Solid State Chem., 2, 137-143 (1970); and Suchow, L. and Kokta, M. (private communication); Chemistry Department, Newark College of Engineering, Newark, N.J.

4. Wyckoff, W. C., Crystal Structures, 2nd Edition, Interscience Publishers, New York, Vol. 1, (1964) p. 85.

5. Cotton and Wilkinson, Advanced Inorganic Chemistry, Interscience Publishers, (1967), p. 51.

6. Martin, D. H. Magnetism in Solids, The M.I.T. Press, Massachusetts Institute of Technology, Cambridge, Massachusetts.

7. Suchow, L. and Stemple, N. R., J. Electrochem., Soc., 110, 1870, (1963), and 111, 191 (1964).

8. Patrie, M., Flahaut, J., and Domange, L., Comptes Rendus Acad Sc., Paris 258, 2585 (1964).

9. Longo, J. M., and Raccah, P. M., Materials Research Bulletin 2, 541 (1967).

10. Suchow, L., and Ando, A. A., J. Solid State Chem., 2, 156-159 (1970).

11. Meisel, K., Z. Anorg. Allgem. Chem., 240, 300 (1939)

12. Holtzberg, F., McGuire, T. R. J. Appl. Phys., 35, 1033 (1964).

13. Holtzberg, F., Methfessel, S., J. Appl. Phys., 37, 1433 (1966).

14. Ferraro, J. R., Labonville, P., Chemistry Division Argonne National Laboratory, (1971) p. 176

15. Wyckoff, W. C., Crystal Structures, 2nd Edition, Interscience Publishers, Vol. 11, (1964), P. 161.

16. Methfessel, S., Kneller, E., Appl. Phys. Letter, 2,

17. Bonder, R. E., Steinfink, H., Metallurgy Session M, Third Conference on Rare Earth Research, Ames, Iowa, 1965.

18. Gambino, R. J., J. Less-Common Metals, 12, 344-352 (1967).

19. Flahaut, J., Domange, L., Guittard, M., Pardo, M., and Patrie, Comptes Rendus Acad. Sc., 257, 1530-1533 (1963).

20. Spedding, F. H., Gschneidner, K. A., and Daane, A. H., J. Amer. Chem. Soc., 80, 4499-4503 (1958).

21. Helms, A., Klemm, W., Z. Anorg. Allgem. Chem. 242, 201 (1939).

22. Gschneidner, Jr., K. A., Rare Earth Alloys, Van Nostrand, Princeton, New Jersey, 1961, p. 137.

23. Hulliger, F., Vogt, O., Solid State Communications, 8, 771-772 (1970).

24. Mass, K. E., Naturwissensch, 55, 489 (1968).

25. Holtzberg, F., McGuire, T. R., J. Appl. Phys. 35, (3), 1033-1038 (1964).

26. Vickery, R. C., Muir, H. M., Rare Earth Research, Macmillan Company, 1961, p. 223.

27. Benacerraf, A., and Guittard, M., Compt. Rend., 248, 1672, 2012 (1959).

28. Iandelli, A. and Kleber, E. V., (ed.), Rare Earth Research, Arrowhead Research Conf., Lake Arrowhead, Calif., 1960, MacMillan, New York, 1961.

29. McMasters, O. D., and Gschneidner Jr., K. A., Trans. AIME, Inst. Metals Div. Spec. Rept. Ser., 10 (13), 93 (1964).

30. Bruzzone, G., Ruggiero, A. F., and Olcese, Atti. Acad. Nazl. Lincei, Rend., Classe Sci. Fis. Mat. Nat., 36, 66 (1964).

31. Craven, W. E., and Ostertag, W., Proc. 7th Rare-Earth Conf., Coronado, Calif. Oct. 28-30 (1968).

32. Goncharova, E. V., Zhuze, V. P., Zhvkova, T. B., Smirnov, I. A., and Shadrichev, *Soviet Physics-Solid State*, <u>10</u>, 1052 (1968).

33. Wang, R., and Steinfink, H., *Inorg. Chem.*, <u>6</u>, 1685 (1969).

34. Eatough, N. L., and Hall, H. T., *Inorg. Chem.*, <u>8</u>, 1439 (1969).

35. Wang, R., and Steinfink, H., *Inorg. Chem.*, <u>6</u>, 1689 (1967).

36. Eatough, N. L., and Hall, H. T., *Inorg. Chem.*, <u>8</u>, 1445 (1964).

37. Hohnke, D., and Parthé, E., *Acta Cryst.*, <u>21</u>, 435 (1966).

38. Ono, S., Despault, J. G., Calvert, L. D., and Taylor, J. B., *J. Less-Common Metals*, <u>22</u>, 57 (1970).

39. Gambino, R. J., *J. Less-Common Metals*, <u>12</u>, 344 (1967).

40. Wells, A. F., *Structural Inorganic Chemistry*, Third Edition, Oxford University Press, London, 1967, P. 1013.

41. Wells, A. F., *Structural Inorganic Chemistry*, Third Edition, Oxford University Press, London, 1967, P. 513.

42. Wyckoff, W. C., *Crystal Structures*, 2nd. Edition, Vol. I, Interscience Publishers, 1963, P. 128.

43. Wyckoff, W. C., *Crystal Structures*, 2nd. Edition, Vol. I, Interscience Publishers, 1963, P. 88-89.

44. Suchow, L., Witzen, M. B., and Stemple, N. R., *Inorg. Chem.* <u>2 (3)</u>, 441 (1963).

45. Asprey, L. B., Keenan, T. K., and Krose, F. H., *Inorg. Chem.*, <u>3</u>, 1140 (1964).

46. Passerini, L., *Gazz. Chim. Ital.*, <u>58</u>, 776 (1928).

47. Dieke, G. H., *Spectra and Energy Levels of Rare-Earth Ions in Crystals*, Interscience Publishers, 1968, p. 23.

48. Cotton and Wilkinson, *Advanced Inorganic Chemistry*, 2nd Edition, Interscience Publishers, (1966) P. 1056.

49. Barns, J. C., _J. Chem. Soc._, London, Oct., Nov., 3880 (1964).

50. Bauman, _Absorption Spectroscopy_, John Wiley & Sons, Inc., New York, 1962, P. 107.